

Amplification of Fluctuations in a Spinor Bose Einstein Condensate

S. R. Leslie^{1*} and J. Guzman^{1,2}, M. Vengalattore¹, J. D. Sau¹, M. L. Cohen^{1,2}, D. M. Stamper-Kurn^{1,2}

¹*Department of Physics, University of California, Berkeley CA 94720*

²*Materials Sciences Division, Lawrence Berkeley National Laboratory, Berkeley, CA 94720*

(Dated: October 31, 2018)

Dynamical instabilities due to spin-mixing collisions in a ⁸⁷Rb $F = 1$ spinor Bose-Einstein condensate are used as an amplifier of quantum spin fluctuations. We demonstrate the spectrum of this amplifier to be tunable, in quantitative agreement with mean-field calculations. We quantify the microscopic spin fluctuations of the initially paramagnetic condensate by applying this amplifier and measuring the resulting macroscopic magnetization. The magnitude of these fluctuations is consistent with predictions of a beyond-mean-field theory. The spinor-condensate-based spin amplifier is thus shown to be nearly quantum-limited at a gain as high as 30 dB.

Accompanied by a precise theoretical framework and created in the lab in a highly controlled manner, ultracold atomic systems serve as a platform for studies of quantum dynamics and many-body quantum phases. Among these systems, gaseous spinor Bose Einstein condensates [1, 2, 3, 4, 5], in which atoms may explore all sub-levels of a non-zero hyperfine spin F , provide a compelling opportunity to access the static and dynamical properties of a magnetic superfluid [6, 7, 8, 9, 10].

We previously identified a quantum phase transition in an $F = 1$ spinor Bose Einstein condensate between a paramagnetic and ferromagnetic phase [9]. This transition is crossed as the quadratic Zeeman energy term, of the form qF_z^2 , is tuned through a critical value $q = q_0$; here, F_z is the longitudinal (\hat{z} axis) projection of the dimensionless vector spin operator \mathbf{F} . Accompanying this phase transition is the onset of a dynamical instability in a condensate prepared in the paramagnetic ground state, with macroscopic occupation of the $|m_z = 0\rangle$ magnetic sublevel [11, 12, 13]. This instability causes transverse spin perturbations to grow exponentially, producing atoms into the $|m_z = \pm 1\rangle$ sublevels. In contradiction with the mean-field prediction that the paramagnetic state should remain stationary because it lacks fluctuations by which to seed the instability, experiments revealed the spontaneous magnetization of such condensates after they were rapidly quenched across the phase transition.

In this Letter, we investigate the spin fluctuations that become amplified by the spin-mixing instability. In particular, we test whether these fluctuations correspond to quantum noise, i.e. to the zero-point fluctuations of quantized spin excitation modes that become unstable. For this, we use the spin-mixing instability as an amplifier, evolving microscopic quantum fluctuations into measurable macroscopic magnetization patterns. We present two main results. First, we characterize the spin-mixing amplifier and demonstrate its spectrum to be tunable by varying the quadratic Zeeman shift. This spectrum compares well with a theoretical model that accounts for the inhomogeneous condensate density and for magnetic dipole interactions. Second, we measure precisely the

transverse magnetization produced by this amplifier at various stages of amplification, up to a gain of 30 dB in the magnetization variance. This magnetization signal corresponds to the amplification of initial fluctuations with a variance slightly greater than that expected for zero-point fluctuations.

Descriptions of the dynamics of initially paramagnetic spinor condensates [11, 12, 14, 15, 16, 17] have focused on the effects of the quadratic Zeeman shift and of the spin-dependent contact interaction. The latter interaction has the mean-field energy density $c_2 n(\mathbf{F})^2$, and, with $c_2 = 4\pi\hbar^2\Delta a/3m < 0$, favors a ferromagnetic state; here, $\Delta a = (a_2 - a_0)$ where $a_{F_{\text{tot}}}$ is the s -wave scattering length for collisions between particles of total spin F_{tot} [1, 2] and m is the atomic mass. Excitations of the uniform condensate include both the scalar density excitations and also two polarizations of spin excitations with a dispersion relation given as $E_s^2(\mathbf{k}) = (\varepsilon_k + q)(\varepsilon_k + q - q_0)$, where $\varepsilon_k = \hbar^2 k^2/2m$ and $q_0 = 2c_2 n$. For $q > q_0$, spin excitations are gapped ($E_s^2 > 0$), and the paramagnetic condensate is stable. Below this critical value, the paramagnetic phase develops dynamical instabilities, defined by the condition $E_s^2 < 0$, that amplify transverse magnetization. The dispersion relation defines the spectrum of this amplification, yielding a wavevector-dependent time constant for exponential growth of the power in the unstable modes, $\tau = \hbar/2\sqrt{|E_s^2|}$.

The unstable regime is divided further into two regions. Near the critical point, reached by a “shallow” quench to $q_0/2 \leq q < q_0$, the fastest-growing instability occurs at zero wavevector, favoring the “light-cone” evolution of magnetization correlations at ever-longer range [11]. For a “deep” quench, with $q < q_0/2$, the instabilities reach a maximum growth rate of $1/\tau = q_0/\hbar$. The non-zero wavevector of this dominant instability sets the size of magnetization domains produced following the quench.

Experimentally, we characterize the spectrum of this amplifier by seeding it with broadband noise and then measuring precisely the spectrum of its output. Similar to previous work [9], we produce condensates of $N_0 = 2.0 \times 10^6$ ⁸⁷Rb atoms, with a peak density of $n = 2.6(1) \times 10^{14} \text{ cm}^{-3}$ and a kinetic temperature of

$\simeq 50$ nK, trapped in a linearly polarized optical dipole trap characterized by trap frequencies $(\omega_x, \omega_y, \omega_z) = 2\pi \times (39, 440, 4.2) \text{ s}^{-1}$. Taking $\Delta a = -1.4(3) a_B$ [18], with a_B being the Bohr radius, the spin healing length $\xi_s = (8\pi n |\Delta a|)^{-1/2} = 2.5 \mu\text{m}$ is larger than the condensate radius $r_y = 1.6 \mu\text{m}$ along the imaging axis (\hat{y}). Thus, the condensate is effectively two-dimensional with respect to spin dynamics. For this sample, $q_0 = 2c_2 \langle n \rangle = h \times 15 \text{ Hz}$ given the maximum \hat{y} -axis column-averaged condensate density \tilde{n} .

The quadratic Zeeman shift arises from the application of both static and modulated magnetic fields. A constant field of magnitude B , directed along the long axis of the condensate, leads to a quadratic shift of $q_B/h = (70 \text{ Hz/G}^2) B^2$. In addition, a linearly polarized microwave field, detuned by $\delta/2\pi = \pm 35 \text{ kHz}$ from the $|F=1, m_z=0\rangle$ to $|F=2, m_z=0\rangle$ hyperfine transition, induces a quadratic (AC) Zeeman shift of $q_\mu = -\hbar \Omega^2 / 4\delta$ where Ω is the Rabi frequency for the driving field.

The condensate is prepared in the $|m_z=0\rangle$ state using rf pulses followed by application of a 6 G/cm magnetic field gradient that expels atoms in the $|m_z=\pm 1\rangle$ states from the optical trap [9]. This preparation takes place in a static 4 G field and with no microwave irradiation, setting $q = q_B + q_\mu > q_0$ so that the paramagnetic condensate is stable. Next, we increase the microwave field strength to a constant value, corresponding to a Rabi frequency in the range of $2\pi \times (0 - 1.5) \text{ kHz}$, to set q_μ . To initiate the instability, we ramp the magnetic field over 5 ms to a value of $B = 230 \text{ mG}$ (giving $q_B/h = 7.6 \text{ Hz}$). During separate repetitions of the experiment (for different values of q_μ), the quadratic Zeeman shift at the end of the ramp was thus brought to final values q_f/h between -2 and 16 Hz.

Following the quench, the condensate spontaneously develops macroscopic transverse magnetization, saturating within about 110 ms to a pattern of spin domains, textures, vortices and domain walls [9]. Using a 2-ms-long sequence of phase-contrast images, we obtain a detailed map of the column-integrated magnetization $\tilde{\mathbf{M}}$ at a given time after the quench [19, 20]. The experiment is then repeated with a new sample.

The observed transverse magnetization profiles of spinor condensates (Fig. 1) confirm the salient features predicted for the spin-mixing amplifier [27]. The variation of the amplifier's spatial spectrum with q_f is reflected in the characteristic size l_d of the observed spin domains, taken as the distance from the origin at which the magnetization correlation function,

$$G(\delta\mathbf{r}) = \frac{\sum_{\mathbf{r}} \tilde{\mathbf{M}}(\mathbf{r} + \delta\mathbf{r}) \cdot \tilde{\mathbf{M}}(\mathbf{r})}{(g_F \mu_B) 2 \sum_{\mathbf{r}} \tilde{n}(\mathbf{r} + \delta\mathbf{r}) \tilde{n}(\mathbf{r})}, \quad (1)$$

acquires its first minimum; here $g_F \mu_B$ is the atomic magnetic moment. This characteristic size increases with increasing q_f (Fig. 2). For $q_f/h \geq 9 \text{ Hz}$, the magnetization

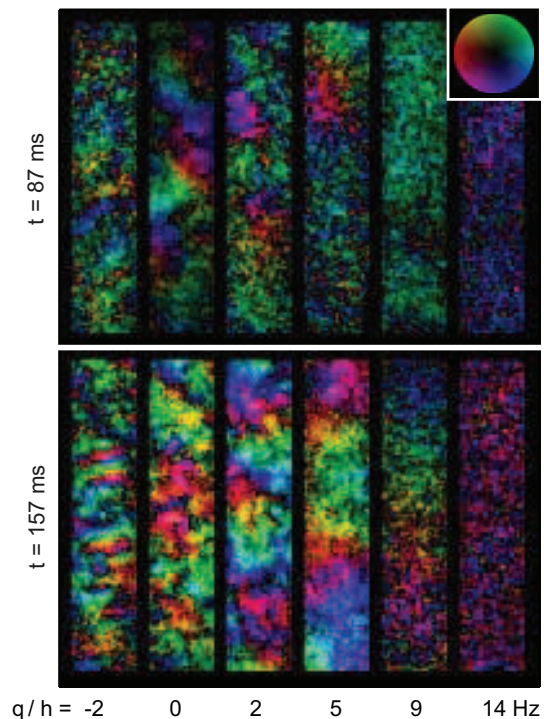


FIG. 1: Transverse magnetization produced near the condensate center after 87 ms (top) and 157 ms (bottom) of amplification at variable quadratic Zeeman shift q_f . Magnetization orientation is indicated by hue and amplitude by brightness (color wheel shown). The characteristic spin domain size grows as q_f increases. The reduced signal strength for $q_f/h \geq 9 \text{ Hz}$ reveals the lower temporal gain of the spin-mixing amplifier.

features become long ranged and, thus, dominated by residual magnetic field inhomogeneities ($< 2 \mu\text{G}$).

The data also confirm the distinction between deep and shallow quenches. The spatially averaged magnetization strength during the amplification, quantified by $G(0)$ at $t = 87 \text{ ms}$ after the quench, is found to be constant for $0 < q_f/h < 6 \text{ Hz}$, reflecting that the temporal gain of the amplifier is uniform over $0 \leq q \leq q_0/2$ [11]. For shallow quenches, with $q_f/h \geq 7 \text{ Hz}$, the measured magnetization decreases, reflecting a diminishing gain with increasing q_f up to the transition point.

While the above observations are consistent with theoretical predictions, we note the unexpected outcome of quenches to negative values of q_f . Such quenches revealed a diminished amplifier gain, resulting in a complete suppression of the growth of magnetization for $q_f/h \leq -7 \text{ Hz}$. We are unable to account for this behavior.

Having characterized the spin-mixing amplifier, let us consider the source of its input signal. For this, we develop a quantum field description of the spin-mixing instability [11], working in the polar spin basis, where $\hat{\phi}_{n,k}$ is the annihilation operator for atoms of wavevector k in the zero-eigenvalue states of $F \cdot \mathbf{n}$. Treating a uni-

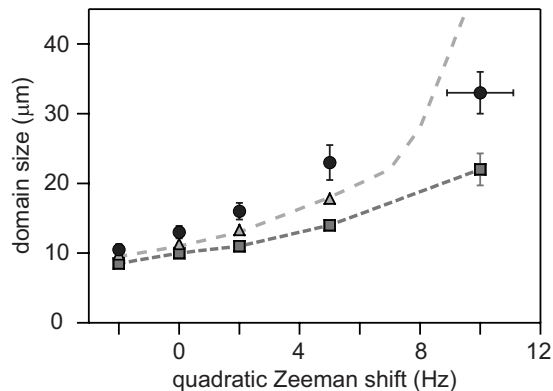


FIG. 2: Characteristic domain size after 87 ms of amplification at variable quadratic Zeeman shift q_f . Data (circles) are averages over 5 experimental repetitions; error bars are statistical. Horizontal error bar reflects systematic uncertainty in q_f . Predictions based on numerical simulations for $|\Delta a| = 1.45 a_B$ [8] (squares) and $1.07 a_B$ [21] (triangles) are shown, with error bar reflecting systematic uncertainty in the atomic density.

form condensate within the Bogoliubov approximation, one defines mode operators $\hat{b}_{n,k} = u\hat{\phi}_{n,k} + v\hat{\phi}_{n,-k}^\dagger$ for the two polarizations of transverse ($n \in \{x, y\}$) spin excitations. The spin-dependent many-body Hamiltonian H_s is then approximated as representing two independent parametric amplifiers:

$$H_s = -\frac{i}{2} \sum_k |E_s(k)| \left(b_{x,k}^2 - b_{x,k}^{\dagger 2} + b_{y,k}^2 - b_{y,k}^{\dagger 2} \right). \quad (2)$$

The parametric amplifiers serve to squeeze the initial state in each spin excitation mode, amplifying one quadrature of $b_{n,k}$ (its real part) and de-amplifying the other.

The above treatment may be recast in terms of spin fluctuations atop the paramagnetic state: fluctuations of the transverse spin, represented by the observables F_x and F_y , and fluctuations in the alignment of the spinor, represented by the components N_{yz} and N_{xz} of the spin quadrupole tensor. We identify the Bogoliubov operators defined above as linear combinations of these observables. Based on this identification, we draw two conclusions. First, an ideally prepared paramagnetic condensate is characterized by quantum fluctuations of the Bogoliubov modes. In the linear regime, fluctuations in $b_{x,k}$ ($b_{y,k}$) correspond to projection noise for the conjugate observables F_x (F_y) and N_{yz} (N_{xz}). Second, the dynamical instabilities lead to a coherent amplification of these initial shot-noise fluctuations. While in the present work we observe only the magnetization, in future work both quadratures of the spin-mixing amplifier may be measured using optical probes of the condensate nematicity [22] or by using quadratic Zeeman shifts to rotate the spin quadrature axes.

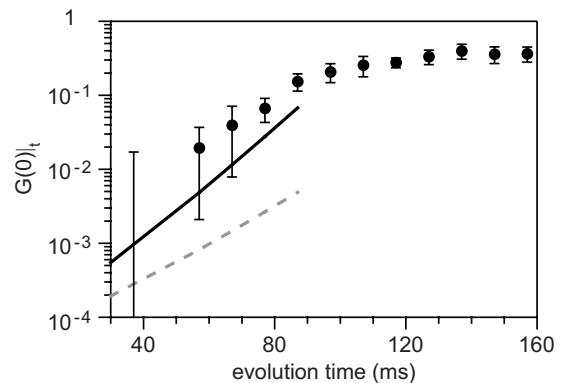


FIG. 3: Temporal evolution of the transverse magnetization variance $G(0)$, evaluated over the central $16 \times 124 \mu\text{m}$ region of the condensate and averaging over 8 experimental repetitions; error bars are statistical. The contribution to $G(0)$ from imaging noise was subtracted from the data. Predictions from numerical calculations for $|\Delta a| = 1.45 a_B$ and $1.07 a_B$ are shown as black and gray lines, respectively.

To test the validity of this quantum amplification theory, we determine $G(0)$ over the central region of the condensate after different intervals of amplification (Fig. 3). We consider the linear-amplification theory to be applicable for $t \leq 90$ ms, and, following Ref. [11], perform a least-squares fit to a function of the form

$$G(0)|_t = G(0)|_{t_m} \times \sqrt{t/t_m} e^{(t-t_m)/\tau} \quad (3)$$

Here τ is the time constant characterizing the growth rate of the magnetization variance and $G(0)|_{t_m}$ is the value of $G(0)$ at time $t_m = 77$ ms.

To compare our measurements to the amplifier theory outlined above, we performed numerical calculations of $G(0)|_t$, taking into account the inhomogeneous density profile; dipolar interactions; proper position-space, rather than momentum-space, spin excitation modes; and quantum fluctuations of the initial state [28]. Such calculations, results of which are shown in Figs. 3 and 4, were performed for several values of the scattering length difference Δa within the range of recent measurements [8, 21]. Our data are consistent with the quantum-limited amplification of zero-point quantum fluctuations in the case that $|\Delta a|$ lies in the upper range of its reported values. Taking τ to be determined instead solely on the basis of our measurements, the magnetization variance is measured to be between 1 and 50 times greater than that predicted by the zero-temperature quantum theory.

Several investigations were performed to identify technical or thermal contributions on top of the expected quantum spin fluctuations of our samples. We place an upper bound on thermal noise by performing a Stern-Gerlach analysis of populations N_\pm in the $|m_z = \pm 1\rangle$ states just after the quench. Obtaining $N_\pm \leq 3 \times 10^2$ and assuming an incoherent admixture of Zeeman sublevels, the thermal contribution to $G(0)|_0$ is below $(2N_\pm/N_0) =$

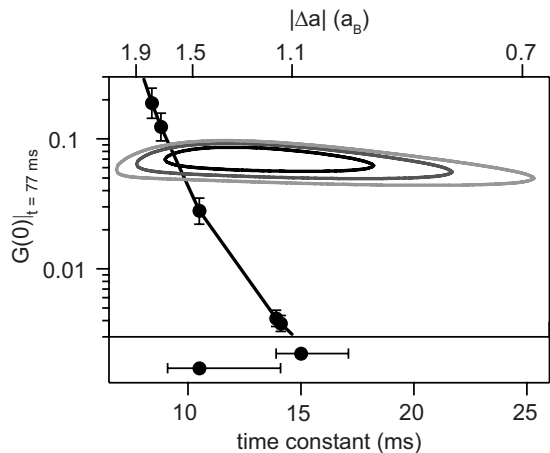


FIG. 4: The magnetization variance $G(0)_{t_m}$ at $t_m = 77$ ms and exponential time constant τ of the amplifier, obtained by fitting data in Fig. 3, are indicated by contours of the 1, 2, and 3 σ confidence regions using a χ^2 test. Predictions from numerical calculations of the zero-temperature quantum amplification theory, assuming different values of $|\Delta a|$, are shown (circles and interpolating line). Error bars reflect systematic uncertainty in q_f and in the condensate density. Time constants corresponding to reported values for $|\Delta a|$ are indicated at bottom.

3×10^{-4} . We confirmed that our results are insensitive to variations in the gradient strength, duration, and orientation used during the initial state preparation, and also to the delay (varied between 0 and 110 ms) between this preparation and the initiation of the spin amplifier. We checked against technical noise that would induce extrinsic Zeeman transitions during the experiment, finding that a condensate starting in the $|m_z = -1\rangle$ state remained so for evolution times up to 400 ms following the quench. Altogether, these results suggest that paramagnetic samples were produced with a near-zero spin temperature, to which the quantum amplification theory may be expected to apply.

The microwave fields used to vary the quadratic Zeeman shift cause a slight mixing between the $F = 1$ and $F = 2$ hyperfine levels. We checked for the influence of this admixture by varying the relative contributions of the static and modulated field contributions to the final quadratic Zeeman shift $q_f = q_B + q_\mu$. As expected given the small value of $(\Omega/\delta)^2 < 10^{-3}$, no variation in the magnetization evolution for constant q_f was observed.

It remains uncertain whether the zero-temperature amplifier theory should remain accurate, out to a gain in the magnetization variance as high as 30 dB, in a non-zero temperature gas subject to constant heating and evaporation from the finite-depth optical trap. Indeed, previous work showed a strong influence of the non-condensed gas on spin dynamics in a two-component gaseous mixture [23]. We compared the amplification of magnetization at kinetic temperatures of 50 and 85 nK,

obtained for different optical trap depths. We observed no variation, but note that the condensate fraction was not substantially varied in this comparison.

In this work, we have demonstrated near-quantum-limited amplification of magnetization fluctuations using dynamical instabilities in a spinor Bose gas. Just as the demonstration of matter-wave amplification in scalar condensates suggested a host of applications [24, 25, 26], the spin-mixing amplifier may serve as an important experimental tool in probing systems with multiple degrees of freedom or in spatially resolved magnetometry [20].

We acknowledge insightful discussions with J. Moore and S. Mukerjee and experimental assistance from C. Smallwood. This work was supported by the NSF, the David and Lucile Packard Foundation, DARPA's OLE Program, and the U.S. Department of Energy under Contract No. DE-AC02-05CH11231. Partial personnel and equipment support was provided by the Division of Materials Sciences and Engineering, Office of Basic Energy Sciences. S.R.L. acknowledges support from the NSERC.

* Electronic address: sleslie@berkeley.edu

- [1] T.-L. Ho, Phys. Rev. Lett. **81**, 742 (1998).
- [2] T. Ohmi and K. Machida, J. Phys. Soc. Jpn. **67**, 1822 (1998).
- [3] J. Stenger et al., Nature **396**, 345 (1998).
- [4] H. Schmaljohann et al., Phys. Rev. Lett. **92**, 040402 (2004).
- [5] M.-S. Chang et al., Phys. Rev. Lett. **92**, 140403 (2004).
- [6] H.-J. Miesner et al., Phys. Rev. Lett. **82**, 2228 (1999).
- [7] D. Stamper-Kurn et al., Phys. Rev. Lett. **83**, 661 (1999).
- [8] M.-S. Chang et al., Nature Physics **1**, 111 (2005).
- [9] L. Sadler et al., Nature **443**, 312 (2006).
- [10] M. Vengalattore et al., Phys. Rev. Lett. **100**, 170403 (2008).
- [11] A. Lamcraft, Phys. Rev. Lett. **98**, 160404 (2007).
- [12] H. Saito et al., Phys. Rev. A **75**, 013621 (2007).
- [13] W. Zhang et al., Phys. Rev. Lett. **95**, 180403 (2005).
- [14] B. Damski and W. H. Zurek, Phys. Rev. Lett. **99**, 130402 (2007).
- [15] M. Uhlmann et al., Phys. Rev. Lett. **99**, 120407 (2007).
- [16] H. Saito and M. Ueda, Phys. Rev. A **72**, 023610 (2005).
- [17] G. I. Mias et al., Phys. Rev. A **77**, 023616 (2008).
- [18] E. van Kempen et al., Phys. Rev. Lett. **88**, 093201 (2002).
- [19] J. Higbie et al., Phys. Rev. Lett. **95**, 050401 (2005).
- [20] M. Vengalattore et al., Phys. Rev. Lett. **98**, 200801 (2007).
- [21] A. Widera et al., New Journal of Physics **8**, 152 (2006).
- [22] I. Carusotto and E. J. Mueller, J. Phys. B **37**, S115 (2004).
- [23] J. M. McGuirk et al., Phys. Rev. Lett. **91**, 150402 (2003).
- [24] L. Deng et al., Nature **398**, 218 (1999).
- [25] M. Kozuma et al., Science **286**, 2309 (1999).
- [26] S. Inouye et al., Phys. Rev. Lett. **85**, 4225 (2000).
- [27] We measure also the longitudinal magnetization of the condensate, but, consistent with prior observations, find that it remains small ($< 15\%$ of the maximum magnetization)

[28] J.D. Sau et al., to be published